promoting access to White Rose research papers

Universities of Leeds, Sheffield and York
http://eprints.whiterose.ac.uk/

This is the author's version of an article published in **Bioresource Technology**

White Rose Research Online URL for this paper:

http://eprints.whiterose.ac.uk/id/eprint/75964

Published article:

White Rose Research Online
eprints@whiterose.ac.uk

Characterisation of palm empty fruit bunch (PEFB) and pinewood bio-oils and kinetics of their thermal degradation

P. Pimenidou[1*] and V. Dupont[2]

[1]Built Environment Institute, University of Ulster, Newtonabbey, Northern Ireland, BT37 0QB, UK

[2] Energy and Resources Institute, The University of Leeds, Leeds, LS2 9JT, UK

Abstract

Ultimate and proximate analyses and thermal degradation of bio oils from pinewood and palm empty fruit bunches (PEFB) were carried out to evaluate the oils' potential for production of fuels for transport, heat and power generation, and of hydrogen via the calculation of performance indicators. The pinewood and PEFB oils indicated good theoretical hydrogen yields of 13.7 and 15.9 wt% via steam reforming, but their hydrogen to carbon effective ratios were close to zero, and their propensity for fouling and slagging heat exchanger surfaces via combustion was high. Both oils exhibited two phases during mass loss under nitrogen flow at heating rates of 3-9 K min^{-1}, but the kinetics of their thermal degradation from TGA-FTIR analysis indicated different degradation mechanisms that were well reproduced by a nth order reaction model for pinewood and Jander's 3D-diffusion model for PEFB. These findings lead to recommendations on pretreatments prior to the oils' utilisation.

Keywords: pinewood; PEFB; bio-oil; TGA-FTIR; kinetics

1. Introduction

Understanding of the behaviour of biofuels will facilitate their direct application, post-treatment or upgrade. Bio-oils can be generated by gasification or fast pyrolysis of biomass or biomass waste. These fuels have low volatility, low calorific value, high acidity and high viscosity (Bridgwater et al., 1999). Post-treatment of pyrolysis oils by hydrodeoxygenation (Elliot, 2007, Zhao et al., 2009; Qi et al., 2007) can enhance their energetic value, as well as the bio-oils' fractional yield (Wan et al., 2009). Catalytic fast pyrolysis can upgrade bio-oil (Williams 1995, Zhang Q. et al., 2007; Zhang H. et al., 2011). Gasification of bio-oil followed by the Fischer-Tropsch process has been recently carried out to produce biofuels from bio-oil syngas to replace gasoline and diesel (Wang Z. et al., 2007). Liquids of biomass origin such as vegetable oils (Pimenidou et al., 2010a; Marquevich et al., 2001) have been investigated as potential sources of hydrogen or as feedstock for biodiesel or blends of biodiesel (Garcia-Perez, 2010). A high hydrogen purity product can be obtained from waste vegetable oil (Pimenidou et al., 2010b) by sorption enhanced steam reforming and chemical looping reforming 'SE-CLR'. Pimenidou et al. (2010b) showed that the chemical looping reactor could operate with sorption enhancement without external heat input for long periods of time within each cycle while producing hydrogen with a purity exceeding 90 %, evidencing autothermal behaviour. During steam reforming, bio-oils can pyrolyse via evaporation when injected onto the hot catalyst bed as well as via vaporisation (by reacting with the steam).

The current study analysed biofuels prepared via fast pyrolysis (500 °C) from pinewood and palm empty fruit bunches (PEFB). A waste product of the oil palm industry, palm empty fruit bunches are produced in vast quantities in West Africa and Southeast Asia, and 5% of household waste in Western countries like the UK consists of wood (Parfitt, 2002). In the EU,

an average of 7.5 million tonnes of waste wood per annum were reported between 2004 and 2008 (European Commission waste statistics). It is estimated that 4.5 million tonnes of waste wood were produced in the UK in 2003, a quarter of which from the manufacture of panelboards (Nikitas et al., 2005). As panelboard in particular particle board and medium density fibre (MDF) board are already made of recycled wood products, panelboard waste is difficult to recycle and most is sent to landfill (Bonigut and Kerley, 2005) or burnt on site for heat generation. Furthermore the market for particle board and MDF are steadily growing at rates of 2.5 and 6% annually, respectively (Bonigut and Kerley, 2005).

Moisture-free PEFB consists of 38.1 to 59.7 wt% cellulose, 16.8 to 22.1 wt% hemicelluloses, and 10.5 to 18.1 wt% lignin (Abdullah et al., 2008). Pinewood has a cellulose content of ca. 40 wt%, and roughly equal proportions of hemicellulose and lignin (around 30 wt%).

The utilisation of PEFB oil for hydrogen production via steam reforming was demonstrated in previous work (Lea-Langton et al., 2011). Thermogravimetric analyses of the pyrolysis of wood or palm wood for biomass fuels production have already been conducted (Reina et al., 1998; Luangkiattikhun et al., 2008; Idris et al., 2010), as have decomposition analyses of pyrolysis oils (Qiang et al., 2010; Dou et al., 2007; Garcia–Perez et al., 2007, 2010) or biofuels such as crude glycerol (Dou et al., 2009). Sukiran et al (2009) studied the effects of PEFB biomass particle size and the parameters of the fast pyrolysis process on bio-oil properties and Abdullah et al. (2008, 2011) investigated the effect of pre-treating the biomass by various methods of water washing on the properties of PEFB bio-oils produced by fast pyrolysis.

The present study aimed to characterise bio-oils from pinewood and palm empty fruit bunches to generate numerical indicators of their potential for upgrading to transport and combustion fuels, and to hydrogen. Given the importance of thermal degradation in refinery upgrading, combustion and hydrogen production processes, the kinetics of the thermal degradation behaviour of the oils was also investigated.

2. Materials and methods

2.1 Materials' characterisation

The pinewood and palm empty fruit bunch bio-oils were obtained from BTG Biomass Technology Group BV, The Netherlands, and BTG via Genting Bio-oil Sdn. Bhd., Malaysia, respectively. Determination of CHNS content in the bio-oils by elemental analysis was carried out with a FlashEA 1112 Series CE Instrument by ThermoFisher Scientific. Inorganic elements in the oils were determined by inductively coupled plasma mass spectrometry (Perkin Elmer SCIEX Elan 900) after sample digestion using a microwave digester (Anton Paar Multiwave 3000). The preparation for digestion required about 7 ml HNO_3, 1 ml HCl and 2 ml H_2O_2 reagents to be added into 150 mg of sample and blank, and the mixtures to be left 5–10 min to react before loaded in the microwave digester to undergo a 4-step power programme (2 min at 1400 W-15 min at 900 W, 15 min at 1400 W ending with 15 min at 0 W fan setting 3). After digestion, the samples were left to cool down in a fume cupboard, and then diluted with ultrapure water (100 ml) before transferring to the ICP-MS instrument.

Water content was determined using a METLER Toledo V20 volumetric type of Karl Fischer titrator. Suspended solids in the bio-oils were removed by filtration through Whatman

1001-070 filter paper prior to water and inorganic element analysis. The oxygen mass fraction was calculated as one minus the sum of all the organic and inorganic elements mass fractions. The values were then converted to mol fractions.

Volatiles, carbon residue and ash content were determined using a Stanton Redcroft TGA-TGH 1000.

Higher heating values (HHV$_{b.c.}$) were determined using a 6200 Oxygen Bomb calorimeter (Parr Instrument Co). The values measured by bomb calorimetry were then compared using two empirical equations that correlate HHV to the wt% of carbon (C_C), hydrogen (C_H), sulphur (C_S), nitrogen (C_N), oxygen (C_O) and ash (C_A) in the fuel. Zhu et al. (2005) derived their correlation from fitting the HHV of over 28 fuels, 14 of which biomass as follows:

$$SR = \left(\frac{C_C}{12} + \frac{C_H}{4} - \frac{C_O}{32} \right) \times \left(1 + \frac{79}{21} \right) \times \left(1 - \frac{C_A}{100} \right) \times \frac{28.84}{100} \quad (1)$$

$$HHV(Zhu) = \frac{SR}{0.31} \quad (2)$$

Channiwala and Parikh (2001) correlated HHV for 225 fuels including fossil and biomass and validated the correlation for an additional 50:

$$HHV(Chan) = 0.3491C_C + 1.1783C_H + 0.1005C_S - 0.1034C_O - 0.0151C_N - 0.0211C_A \quad (3)$$

HHVs on a moisture-free basis were calculated via the determination of the formation enthalpy of the as-received 'wet' oils, themselves calculated from the knowledge of the 'wet' HHVs, and the subsequent calculation of the formation enthalpy of the moisture-free 'mf' oils using the water and the dry oil fractions. The 'wet' and 'moisture-free' lower heating values (LHV) of the oils were then determined from their respective HHV values using the

stoichiometry of the combustion reaction of the bio-oils (wet/m.f) and the enthalpy of water vaporisation, as per definition of HHV and LHV.

Analysis of the chemical composition of the bio-oils was performed by using the GC-MS (Gas Chromatography-Mass Spectroscopy). The GC-MS apparatus was a Shimadzu 2010. A Trace GC 2000 TOP (Thermo electron) with a splitless injector and a mass spectrometer Fisons MD800 comprised the GC-MS. The column used for the tested samples was the $25 \text{ m} \times 0.25 \text{ mm}$ RESTEK RTX5ms. Helium was used as the carrier gas, with a flow of 1 ml min^{-1}. The injector volume was 2 μl and the injector temperature was 250 °C. The GC oven programme was 10 min at 35 °C, ramped to 290 °C at 5 °C min^{-1}, held for 15 min. The MS source was at 180 °C with the transfer line at 250 °C.

2.2 TGA-FTIR analysis

As-received 'wet' sample masses of approximately 20 mg were placed in the thermogravimetric analyser's crucible and mass loss was determined during heating from 293 to 1073 K at a constant heating rate (3, 6 and 9 K min^{-1}). The TGA apparatus was connected via a transfer line to a FTIR spectrometer (Nicolet Magna 560) fitted with a Thermo Scientific TGA interface. The IR spectra were used to confirm the loss of gases, in particular carbon dioxide and acetic acid, which are the main constituents of the fuels' complete or incomplete oxidation respectively. The transfer line was maintained at 180 °C and the interface cell oven was at 280 °C. The IR spectra were produced with a resolution of 4 cm^{-1} with 32 scans per spectrum in the wave number range of 4000–400 cm^{-1}. The interval of time between spectra was 60 s. The total data collection time depended on each heating rate, with the maximum and the minimum being 4.5 and 1.5 hours respectively.

2.3 Methodology of the kinetics study of the thermal degradation of the bio-oils

The TGA mass loss conversion values obtained as described in section 2.2 were used for predicting conversion curves over increasing temperatures based on the improved iterative Coats-Redfern method (Urbanovici et al., 1999) for non-isothermal data via the determination of the kinetic parameters. The models tested for the bio oils' thermal degradation in the TGA are represented by the integral rate function 'g' of the normalised mass conversion fraction 'α':

$$\alpha = \left(\frac{m_{t=0} - m_t}{m_{t=0} - m_{t,end}} \right)$$

In the present work, the mass conversion curve with temperature was split into two phases, 'PH1' and 'PH2', representing groups of reactants whose mechanisms of thermal degradation are assumed independent from each other, where the re-normalised mass conversion fractions (α_{PH1} and α_{PH2}) were tested with the models below within the boundaries of each phase:

$$\alpha_{PH1} = \left(\frac{m_{t=0} - m_t}{m_{t=0} - m_{end,PH1}} \right) \text{ and } \alpha_{PH2} = \left(\frac{m_{end,PH1} - m_t}{m_{end,PH1} - m_{end,PH2}} \right)$$

This renormalisation conferred values of 0 and 1 as the respective extrema for each phase.

(i) n^{th} order reaction model : $g(\alpha) = \dfrac{\left(1 - (1-\alpha)^{1-n}\right)}{1-n}$

       with special cases: $n=0$ (power law model, order 1)

       $n=1/2$ (contracting surface model)

       $n=2/3$ (contracting volume or 'shrinking core' model)

(ii)   1D Diffusion model: $g(\alpha) = \alpha^2$

(iii)   3D Diffusion model (Jander equation) : $g(\alpha) = \left(1 - (1-\alpha)^{1/3}\right)^2$

Iterations were repeated until the solution values of E and A no longer changed, exhibiting convergence. To determine the best model for the integral rate function g, the model generating a correlation coefficient (r) closest to 1 was chosen. Finally, the mass loss conversion fraction profile with temperature was calculated using the chosen best-fit kinetic model and compared to the experimental one.

2.4 Calculation of numerical indicators for the direct utilisation or upgrading of the bio-oils

HHV, carbon residue, and ash content are obvious fuel characteristics influencing the efficiency of a combustion process. Recently, the use of biomass as a single or co-firing fuel in power stations has shown increased propensity of biomass to cause slagging, fouling and corrosion of heat exchanger parts compared to coal. Two fouling and slagging indices, namely, the free alkali index (A_f), and the S/(K+Na) molar ratio, are derived from the fuel composition as opposed to that of the ash (Blomberg, 2007) and were therefore calculated for the PEFB and pinewood bio-oils. The equations for the derivation of the free alkali index are given below:

$$A_f = \frac{x \times (Na + K) - 2S}{LHV} \text{ where } x = \min\left(\frac{Ca}{Si}; 1 + \frac{2S}{Na + K}\right)$$

Where Na, K, Ca and Si are in mol/kg of fuel, and LHV is the lower heating value of the fuel in GJ or MJ/kg, the units of A_f are in mol/GJ or mol/MJ.

Blomberg (2007) reported that negative values of A_f, and S/(K+Na) molar ratios higher than 4 have been interpreted to indicate low fouling propensity.

The ultimate analysis and the calculated LHV of the as-received 'wet' and moisture-free oils allowed the determination of A_f, the free alkali index, and of the S/(K+Na) molar ratio.

From the stoichiometry of the steam reforming reaction, the maximum hydrogen yield from the conversion of a '$C_nH_mO_k$' feedstock, e.g. a bio-oil, and water, into CO_2 and H_2 products is $(2n+0.5m-k)$ mol of H_2 per mol of feedstock, according to the balanced steam reforming reaction (SR) below:

SR: $C_nH_mO_k + (2n-k) H_2O \rightarrow nCO_2+(2n+0.5m-k)H_2$
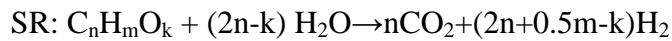
This is equivalent to $100\times2.02\times(2n+0.5m-k)/ (12.01n+1.01m+16k)$ in H_2 wt% of the feedstock.

The effective hydrogen index (EHI), also called 'hydrogen to carbon effective ratio' or $(H/C)_{eff}$ in the literature (Chen et al., 1988), assesses the tendency of a bio-oil to cause coking of zeolite catalyst upon upgrading.

$(H/C)_{eff}=(H-2O-3N-2S)/C$ where H, O, N, S and C are the mol fractions in the fuel.

The maximum hydrogen yield (wt%) and the $(H/C)_{eff}$ were determined for the two bio-oils on a 'wet' basis and a moisture-free basis.

3. Results and discussion

3.1 Characterisation of the bio-oils

3.1.1 Ultimate analysis

Results of the ultimate analysis of organic and inorganic elements are given in Table 1. The organic and inorganic composition of the moisture free ('mf') pine oil was very close to

that found by Garcia-Perez et al. (2010). The PEFB oil exhibited a higher carbon content than that measured by Abdullah et al. (2011) on a moisture free basis (60.0 wt% vs. 41.9 wt%) and lower hydrogen (5.1 wt% vs. 7.8 wt%). The carbon and hydrogen contents were marginally lower (45 vs. 49.7 wt%, and 6.5 vs. 8.0 wt%), and the O content higher (47 vs. 40.3 wt%) than those found by Sukiran et al. (2009), assuming their values were not corrected for moisture, and choosing the bio-oil they produced at 500 ℃. The most significant difference between the PEFB and the pinewood oils' ultimate analysis was in the potassium content, with the PEFB oil exhibiting 0.14 wt% compared to just 0.006 wt% in the pine oil. The PEFB oil had slightly higher carbon and slightly lower oxygen contents than the pinewood oil, which would provide a small advantage for upgrading to transport fuels or direct utilisation in combustion applications.

3.1.2. Proximate analysis

3.1.2.1 Water content

The water content of the filtered oils was 23 wt% and 32 wt% ('wet' basis) for the pinewood and PEFB oils, respectively. Assuming a dry filtration residue of nearly pure carbon (neglecting inorganics content in the residue), solution of the mass and carbon balances for the two as-received 'wet' oils yielded 22.6 and 24.3 wt% for pinewood and PEFB, respectively. The assumption of nearly pure carbon in the residues was later justified by the low ash content of the as-received 'wet' oils (section 3.1.2.2). These water contents were in the expected range for bio-oils (Bridgwater, 1999). The pinewood oil water content was higher than the 18 wt% quoted by Garcia-Perez et al. (2010) for bio-oil from pine pellets. The PEFB oil's water content was slightly higher than the 21.7 wt% and 18.7 wt% quoted by Abdullah (2011) and Sukiran (2009), respectively. The discrepancies in the pyrolysis process used to produce the

oils and their wood origins would account for the differences in water content. Higher water content would increase the cost of preheating and drying the fuel in a combustion application, but would reduce the need for water consumption in a steam reforming process. The 'wet' PEFB oil had a significantly larger suspended solids content than the pinewood oil (24.1 vs. 1.9 wt%). Thus, despite the PEFB oil's higher potential for upgrading and utilisation from its higher C and H contents, its solids content would ultimately pose a larger challenge in injection systems and in small diameter pipes than the pinewood oil, where the risk of blockages would be increased by deposits and sedimentation, respectively.

3.1.2.2 Volatiles, carbon residue and ash content

The carbon residue (including inorganics) from the TGA experiments with the pine oil accounted for 11.79- 13.41 wt% of the initial mass used as seen in the mass loss profiles (Fig. 1). For the pinewood oil, increasing the heating rate between 3 and 9 K min^{-1} decreased the carbon residue, contrary to expectations. The values were comparable to 10.3 wt% quoted by Garcia Perez et al (2010) for pine chips. The ash content of the as-received 'wet' pine oil was 3.78 wt%. For the PEFB oil, the carbon residue accounted for 11.35-15.68 wt% of the initial mass used (Fig.1), since increasing the heating rate caused the carbon residue to increase. Its ash content was 2.43 wt% and thus significantly larger than that reported by Sukiran et al. (2009) of 0.65 wt% for the PEFB oil produced at 500 °C. Comparison between the pinewood and the PEFB oils therefore indicated slightly higher carbon residue but lower ash for the PEFB oil.

3.1.2.3 Heating values

The HHV were 19.8 and 15.6 MJ kg^{-1} for the 'wet' PEFB and pine oils respectively. A higher HHV for the PEFB oil had been anticipated due to its lower O content compared to the

pine oil. The value of 19.8 MJ kg^{-1} for PEFB oil compared well with that measured using bomb calorimetry by Sukiran et al. (2009) for the PEFB bio oil produced at 500 °C (21.4 MJ kg^{-1}). The HHV found in the present study for both PEFB and pine oils are in agreement with those found by Czernik et al. (2004).

The empirical HHV values according to Zhu et al's (2005) correlation for the 'wet' PEFB and pine oils were 16.99 and 14.53 MJ kg^{-1}, respectively, and therefore in significant error with the measurements. Using the correlation of Channiwala and Parikh's (2001), the 'wet' oils' HHV were 18.5 and 16.5 MJ kg^{-1}, respectively, and therefore the difference in measured and empirical values was just over 1 MJ kg^{-1}. Although this difference may seem small, due to the small HHV values, it still accounted for a significant 6% relative error for the 'wet' oils.

The calculation of the HHVs on a moisture-free (mf) basis via the enthalpies of formation yielded 20.1 MJ kg^{-1} for the as-received pine oil. This value is very close to the value of 21.6 MJ kg^{-1} measured by bomb calorimetry by Garcia-Perez et al. (2010) for 'mf' pine pellets bio-oil. The 'mf' HHV of 26.2 MJ kg^{-1} for the as-received PEFB oil was significantly higher than the value of 20.32 MJ kg^{-1} calculated by Abdullah et al. (2011) for the oil collected from their tank (as opposed to the walls) and derived using the empirical correlation by Channiwala and Parikh (2001).

Comparison of the HHV for the moisture-free oils calculated with the empirical correlations according to Zhu et al. (2005) and to Channiwala and Parikh (2011) indicated discrepancies in excess of 3 MJ kg^{-1} for the pine and PEFB oils, representing a 15 and a 11 % error with the measurements, respectively. This would indicate that empirical correlations for HHV can carry significant errors, in particular when applied to elemental compositions deriving from

indirect measurements, such as those of the moisture-free oils, which were corrected from the direct measurements on 'wet' oils.

3.1.3 Chemical analysis

For both bio-oils, several oxygenated compounds were found to be acids, such as acetic acid ($C_2H_4O_2$), phenols, aldehydes, ketones and a small percentage of polyaromatic hydrocarbons by the GC-MS analysis (data not shown). Acetic acid was the main component in both bio-oils followed by 1-hydroxy-2-propanone ($C_3H_6O_2$) for the pine oil and n-hexadenoic (palmitic) acid ($C_{16}H_{32}O_2$) for the PEFB oil.

3.1.4. Numerical Indicators for the direct utilisation or upgrading of the bio oils

3.1.4.1 Indicators for combustion in boilers

The fouling and slagging indicators are listed in Table 1. In all cases, the values were in the range of significant propensity for slagging and fouling. Note that a value for untreated pine (the original biomass, not its pyrolysis oil) was 0.4 mol/GJ using a value of 1 for x (Blomberg, 2006) and therefore, burning the original pinewood biomass would cause less fouling than the bio-oil derived from it. Possibly, more favourable oil properties could be achieved by water washing as described by Abdullah et al. (2008, 2011) and Saddawi et al. (2011).

3.1.4.2 Indicator for hydrogen production

The maximum hydrogen yield (in wt% of the fuel) is listed for the as-received 'wet' PEFB and pine oils in Table 1. The maximum H_2 yields are similar for the two 'wet' oils: ~16 wt% for PEFB and 14 wt% for pine. It is noteworthy that after filtration with Whatman filter paper, the pine oil's maximum H_2 yield decreased only slightly to 13.2 wt%, whereas that of the

PEFB filtered oil fell significantly to 7.3 wt%, due to a significant reduction in its carbon content. In an industrial process of hydrogen production from filtered bio-oil, the carbon separated by filtering would be expected to either be burned to provide the heat necessary for the endothermic steam reforming reaction, or be gasified with steam to provide additional hydrogen yield. Using the calculated water content for the 'wet' oils (dry residue basis), maximum H_2 yields on the basis of the moisture-free oils were determined as 21 and 17.7 wt% for the PEFB and pine oils, respectively (Table 1). Experiments of steam reforming and of chemical looping reforming of the filtered PEFB and pine oils at 600 °C in a packed bed reactor loaded with a Ni/Al_2O_3 catalyst were reported by Lea-Langton et al. (2011). The experiments of Lea-Langton et al. indicated that yield efficiencies (defined by the ratio of measured H_2 production rate to maximum theoretical) of 80% were possible, with fuel conversions of 97% for pine and 89 % for PEFB oil respectively, using only modest steam to carbon molar ratios (2.3 and 2.6, respectively, mf basis).

3.1.4.3 Indicators for upgrading to transport fuels

Carbon residue is considered an indicator of coke forming potential from hydrocarbon feedstock in refineries. Typically carbon residues between 10 and 12 wt%, such as those found for the pine oil, would not be expected to pose significant carbon deposition during refinery upgrading such as catalytic cracking (Sadeghbeigi, 2000), whereas values above 20% are considered problematic. With near 15 wt%, the PEFB oil's carbon residue would be expected to pose challenges for refinery upgrading. Pyrolysis oils can be upgraded to olefins and aromatics by hydrodeoxygenation (HDO) over (most commonly) Mo-supported catalysts, or by catalytic fast pyrolysis over zeolite catalysts (CFP) (Elliot, 2007, Lin and Huber, 2009). The hydrogen to carbon effective ratio (H/C)$_{eff}$ was devised specifically for CFP over zeolite

14

catalysts. A value of $(H/C)_{eff}$ lower than 1 indicates fuels undergoing upgrading tend to cause excessive coking and deactivate the catalyst. Bertero et al. (2011) have recently used the carbon residue and the $(H/C)_{eff}$ in their investigation of pyrolysis temperatures and thermal conditioning on the coking potential of bio-oils. Using TGA, Zhang L. et al. (2011) investigated the effect of the $(H/C)_{eff}$ of model oxygenated compounds of bio-oils and some bio-oils on their conversions to olefins and aromatics as well as the resulting deactivation rate of ZSM-5 catalyst. They found that there was a steady increase in catalyst deactivation and equivalent decrease in conversion to olefins and aromatics as the $(H/C)_{eff}$ decreased from a value of 2. As little as 10% conversion was measured at $(H/C)_{eff}$ of zero, and all the data was closely clustered around a monotonic curve. They concluded that H-deficient feedstock could be hydrogenated to achieve a $(H/C)_{eff}$ of 1.2 for acceptable conversion to olefins and aromatics, thereby underlining the role of hydrogen availability for such a process.

Table 1 lists the $(H/C)_{eff}$ for the two as-received 'wet' oils, revealing values very close to zero, and hence a significant coking tendency for upgrading to olefins and aromatics via catalytic cracking on ZSM-5. According to Zhang et al. (2011), these oils would require an additional feed of 1.2 and 1.1 mol of hydrogen per mol of carbon in the pine and PEFB bio-oils, respectively in order to achieve the nominal $(H/C)_{eff}$ of 1.2.

Whereas HDO relies directly on pure hydrogen gas as a co-reactant in the conversion of bio-oils to transportation fuels, the addition of methanol, acetic acid, or methylacetate to bio-oils with poor $(H/C)_{eff}$ have been shown to increase the $(H/C)_{eff}$ in the ZSM-5 CFP process (Chen et al, 1988). However, this approach would still require periodic catalyst regeneration, as shown by experiments with model compounds (Zhang et al., 2011). The requirement for periodic regeneration after addition of higher H/C fuels to the bio-oils would indicate a good

compatibility with the chemical looping process, which incorporates cyclic oxidation of the catalyst, thereby eliminating carbon deposits (Pimenidou et al., 2010a).

3.2 Thermal degradation mechanism

3.2.1. Pinewood oil

TGA of the as-received 'wet' pinewood oil indicated mass loss that initiated at ambient temperature and reached 80% conversion between 650 and 770 K (Fig. 1). The mass loss vs. temperature curves at the three different heating rates demonstrated two distinct phases, termed phase 'PH1' for the low temperature, low conversion range, and 'PH2' for the medium temperature, high conversion range (Table 2). Previous studies have used the differential thermogravimetric profile with temperature as a method for quantifying the chemical 'macrofamilies' fractions of bio-oils, with the assumption that the thermal degradation of individual families do not interact with one another (Garcia-Perez et al., 2007, 2010). According to Garcia-Perez et al. (2010), the DTG of bio-oil from pine pellets under a heating rate of 10 K min^{-1} decomposed into six macrofamilies; family A, light volatiles with boiling point lower than 100 ℃ (e.g. methanol, acetone, acetyldehyde, hydroxyacetyldehyde), with a peak at 60 ℃; family B, water, acetic acid, acetol, this stretches up to 175 ℃ with a peak at 115 ℃; family C, monophenols and furans from 50 to 235 ℃, with a peak at 160 ℃; family D, levoglucosan and other sugars, from 140 to 315 ℃ with a peak at 230 ℃; family E, lignin derived oligomers, from 200 to 500 ℃, with a peak at 310 ℃; family F, cracking products of oligomers also from 200 to 500 ℃ with a peak at 400 ℃.

Fig. 2 plots the DTG vs. temperature for the two as-received oils for the heating rate of 9 K min^{-1}. The positions of the different families with respect to the previously identified phases

PH1 and PH2 are also shown. For pinewood oil, family A in its entirety, half of B and the first quarter of C were included in PH1, whereas the remainder of B, C, D, E and F were covered in PH2. The DTG curve of the pinewood oil can be compared to that for pine bio-oil obtained by Garcia-Perez et al. (2010). In the latter, the following mass fractions were derived: 0.14(A), 0.29(B), 0.2(C), 0.12(D), 0.19(E) and 0.07(F). Visual comparison with the findings of Garcia-Perez et al.'s allowed qualitative estimates in the present study, which indicated the dominant fraction of A, followed by B and C in decreasing order, and then equal small fractions of D and E followed by the smallest fraction of F.

The main compounds generated during PH1 were water, and the compounds identified by GC-MS: acetic acid (boiling point= 118.1 ^{o}C= 391.1 K), n-propyl acetate (boiling point=102 ^{o}C= 375 K), 2-cyclopenten-1-one (boiling point 337 K =64 ^{o}C). PH1 accounted for mass losses between 42 and 48%. The mass loss in PH2 was attributed to substances such as phenols that pyrolysed within this temperature range. Therefore, the post-treatment of such bio-oils may result in a significant mass loss of the fuel. The mass loss percentage during PH2 for all heating rates was within the range from 35 to 45%. The evaporation of 1-hydroxy-2-propanone (418 K; 145 ^{o}C), tetrahydro- 2,5-dimethoxy-furan (420 K; 147 ^{o}C) and furfural (435 K; 162 ^{o}C) would have occurred in phase PH2.

The final pyrolysis phase was concluded at different temperatures (Table 2) depending on the heating rate. When the heating rate was 3 K min^{-1}, 83% of the initial mass of the pyrolysis oil was thermally decomposed at 942 K; for the 6 K min^{-1} the same mass loss was achieved at 640 K and for the 9 K min^{-1} at 636 K.

The thermogravimetric analysis apparatus was coupled with FTIR because of the complexity of the bio-oils and to assist the interpretation of the TGA runs. In phase PH1 the

17

mass loss was characterised by the release of acetic acid (CH_3COOH), evidencing an evaporation process, whereas phase PH2 saw the release of carbon dioxide (CO_2), an effect of chemical reactions by thermal cracking (de-oxygenation). In Fig. 3, the acetic acid (CH_3COOH) and the carbon dioxide (CO_2) relative intensity curves are plotted over the mass loss curve, in order to relate the gaseous emissions of the complex mixtures of compounds comprising prospective fuels to the respective mass loss phases. It should be noted that the mass losses percentage is read on the left hand side y-axis (primary y-axis), whereas the temperature and the relative intensities of either CO_2 or CH_3COOH are on the right hand side y-axis (secondary y-axis). These species were selected because they had the most intense absorption signals: CH_3COOH (spectra band: 1600-1900 cm^{-1}) and CO_2 (spectral band: 2360-2365 cm^{-1}). The spectral band 3500-4000 cm^{-1} corresponded to O-H stretch which is found in water, phenols and alcohols contained in the bio-oils. Two strong carbonyl (C=O) stretches were produced at 1777 and at 1800 cm^{-1} and are associated with the acetic acid production. Fig. 3 shows that acetic acid started to evolve at 377 K (104 °C) and peaked in the 400-480 K range, corresponding to the end of PH1. The C-O stretching at 2361.9 and 2349.3 cm^{-1} was accompanied by release of CO_2 at 477 K (204 °C). The mass loss of the pinewood oil was accompanied until the end of the test by CO_2 release (Fig. 3), evidencing a cracking process. Therefore the CO_2 release occurring at temperatures above 477 K (204 °C) during PH2 is related to the pyrolysis of the pinewood oil, while the mass loss of 50% (Fig. 1) of the initial sample's mass during PH1 was attributed to the loss of acetic acid and other low boiling point compounds such as water, in agreement with the macrofamilies analysis of the DTG. Such results were common for all three heating rates (3, 6, 9 K min^{-1}) (Fig. 1). Based on the FTIR

spectra, it was noticed that the majority of the detected functional groups were oxygenated compounds.

3.2.2. PEFB oil

The mass loss of the PEFB oil initiated at ambient temperature and reached 80% conversion between 630 and 670 K. Similarly to the TGA of the pinewood oil, the mass loss curves of the PEFB oil at the heating rates of 3, 6 and 9 K min^{-1} were also split in two sections (Table 2). PH1 exhibited mass losses between 20 and 30%, which would have accounted mainly for water losses since the water content of the as-received 'wet' PEFB oil was evaluated at 24 wt% (Table 1), but also acetic acid (Fig. 4). PH2 exhibited mass losses between 60 and 70 %, representing the pyrolysis of the organic content in the oil, accompanied by CO_2 release (Fig. 4). The DTG profile shown in Fig. 2 indicated similar fractions of B, C, D, lower fractions of A and E, and lowest fraction of F. The cracking of the hydrocarbons -C-C-C-C- bonds in the bio-oils and the loss of high temperature volatile organic compounds may account for the mass loss in the temperatures around 500 K in PH2. Octadecanoic acid (stearic acid; $CH_3(CH_2)_{16}COOH$) was one of the main substances contained in the tested PEFB bio-oil samples. A large percentage of the mass loss during PH2 may be attributed to the evaporation of octadecanoic acid as its boiling point is 656 K (383 °C).

3.3. Kinetic analysis of thermal decomposition of PEFB and pinewood bio-oils

Kinetic parameters for PH1 and PH2 are presented in Table 3 for pinewood and PEFB bio-oils. The same table lists the correlation coefficients. The nth order reaction model applied to the renormalized conversions during phases 1 and 2 (α_{PH1} and α_{PH2}) best described the mass loss of the as-received 'wet' pinewood oil.

19

This procedure was supported by the end of PH1 corresponding to the peak of acetic acid intensity by the FTIR. The modelled conversion curves and their respective experimental counterparts are plotted in Fig. 5 for the 9 K min^{-1} experiment. The correlation coefficients were approximately 0.99 and showed an excellent fit with the experimental ones for the 3, 6 and 9 K min^{-1} experiments (Table 3).

In Table 3 the calculated kinetic parameters derived from the iterative Coats-Redfern modelling can be seen for both PH1 and PH2 for the pinewood oil. For PH1, activation energies were in the 64-78 kJ mol^{-1} range, with ln$A$ from 17.6 to 23.3 and reaction orders between 2.3 and 3. There was therefore little effect of the heating rate on the kinetic parameters range.

For the PEFB oil, the 3D Jander diffusion model was found to give the best fit on the experimental data of mass loss in PH1 for heating rates 6 and 9 K min^{-1} and all three heating rates in PH2. The Jander equation for 3D diffusion is a model that assumes solid spherical reactant particles surrounded by a 'sea' (large excess) of another solid, liquid or gas reactant. The formation of a product layer on the spherical solid then acts as a diffusion barrier and controls the rate of product formation (Dickinson and Heal, 1999). The PEFB oil was shown to contain significant suspended solids (24.1 wt%, section 3.1.2.1) compared to the pinewood oil (1.9 wt%). This would explain the better fit of the PEFB oil's conversion curve with Jander's 3D diffusion model. For PH1, the activation energies ranged between 26.9 and 56.6 kJ mol^{-1}, although the lower value corresponded to a different model (n^{th} order reaction) and lowest heating rate. PH2 was modelled with lower activation energies (15-4-20.3 kJ mol^{-1}). Activation energies with low values (e.g. below 30 kJ mol^{-1}) indicate a physical process is

taking place, which would correspond to melting or evaporation of the high boiling point components in the bio-oil.

Correlation coefficients (r) of above 0.986 were produced. The 3 K min^{-1} run was modelled using a single phase, resulting in the very high correlation coefficient of 0.996. These high correlation coefficients translated into curves of modelled conversion vs. temperature that were very close to the experimental ones for the 9 K min^{-1} heating rate (Fig. 5).

4. Conclusions

Ultimate and proximate analyses of PEFB and pinewood bio-oils indicated that their direct utilisation as combustion fuels, feedstock for upgrade to transport fuels or hydrogen via steam reforming would pose significant technical challenges without pre-treatment for metal content and solids removal, or hydrogen addition. The conversion vs. temperature curve of the PEFB and pinewood oils were best fitted with Jander's 3D-diffusion equation, and the nth order reaction model, reflecting the two oils' high and low suspended solids content, respectively. The decomposition occurred in two phases identified both via modelling and by the evolution of acetic acid and CO_2, respectively.

Nomenclature

α	normalised mass loss conversion fraction for a whole TGA run
$\alpha_{PH1}, \alpha_{PH2}$	re-normalised mass loss conversion fractions over phases 1 and 2.
β	heating rate (K min^{-1})
A	pre-exponential factor in Arrhenius expression of rate constant
A_f	free alkali index
CFP	Catalytic Fast Pyrolysis
E	activation energy in Arrhenius expression of rate constant (kJ mol^{-1})
PEFB	palm empty fruit bunches
EHI	effective hydrogen index (also called hydrogen to carbon effective ratio)
FTIR	Fourier Transform Infra red Spectroscopy/Analyser
g	integral function of conversion (different equation according to different model)
GC-MS	Gas chromatography coupled with mass spectrometry/analyser
$(H/C)_{eff}$	Hydrogen to carbon effective ratio (also called effective hydrogen index)
HDO	Hydrodeoxygenation
HHV	higher heating value (MJ kg^{-1})
ICP-MS	inductively coupled plasma mass spectrometry/analyser
m_t	sample mass in the TGA at time t.
n	Reaction order in reaction order model
PH1	1st phase of mass loss in TGA (low temperature/low conversion)
PH2	2nd phase of mass loss in TGA (medium temperature/high conversion)
TGA	Thermogravimetric analysis/analyser

References

Abdullah N., Gerhauser H., 2008. Bio-oil derived from empty fruit bunches. Fuel. 87, 2606-2613

Abdullah N., Sulaiman, F., and Gerhauser, H., 2011. Characterisation of Oil Palm Empty Fruit Bunches for Fuel Application. J. Phys. Sci. Vol 22(1) 1-24.

Ahmaruzzaman M., D.K. Sharma. 2005. Non-isothermal kinetic studies on co-processing of vacuum residue, plastics, coal and petrocrop. J. Anal. Appl. Pyrolysis. 73, 263-275.

Aho A., Kumar N., Eranen K., Salmi T., Hupa M., Murzin D.Y., 2008. Catalytic pyrolysis of woody biomass in a fluidized bed reactor: Influence of the zeolite structure. Fuel, 87, 2493-2501.

Bertero M., de la Puente, G, Sedran, U., 2011. Effect of pyrolysis temperature and thermal conditioning on the coke forming potential of bio-oils. Energy Fuels, 25, 1267-1275.

Blomberg, T., 2006. Materials and Corrosion, 57(2), 170-175.

Blomberg, T, 2007. ECI Symposium Series, Volume RP5: Proceedings of 7th International Conference on Heat Exchanger Fouling and Cleaning - Challenges and Opportunities, Editors Hans Müller-Steinhagen, M. Reza Malayeri, and A. Paul Watkinson.

Bonigut, J., and Kerley, V. C., 2005. Options for increasing the recovery of panelboard waste. The Waste and Resources Action Programme (WRAP). ISBN: 1-84405-179-X

Bridgwater, A., V., Meier, D., Radlein, D., 1999. An Overview of fast pyrolysis of biomass. Org. Geochem. 30, 1479-1493.

Channiwala, S. A. and Parikh, P. P., 2001. A unified correlation for estimating HHV of solid, liquid and gaseous fuels. Fuel, 81, 1051–1063.

Chen, N. Y., Walsh, D. E., and Koenig, I. R. Chapter 24. Fluidized Bed Upgrading of Wood Pyrolysis Liquids and Related Compounds. p 277-289. Pyrolysis Oils from Biomass: Producing, Analyzing, and Upgrading. Editors J. Soltes and Thomas A. Milne. American Chemical Society, Washington, DC, 1988.

Czernik S., Bridgwater A.V., 2004. Overview of applications of biomass fast pyrolysis oil. Energy Fuels. 18, 590- 598.

Dickinson, C. F., Heal, G. R., 1999. Solid-liquid diffusion controlled rate equations. Thermochim. Acta, 340-341, 89-103.

Dou B., Dupont V., Williams P. T., Chen, Ding Y, 2009. Thermogravimetric kinetics of crude glycerol. Bioresour. Technol. 100, 2613-2620.

Dou B., Park S., Lim S., Yu T. U., Hwang J., 2007. Pyrolysis characteristics of refuse derived fuel in a pilot- scale unit. Energy Fuels. 21, 3730- 3734

Elliott, D.C., 2007. Hystorical developments in hydroprocessing bio oils. Energy Fuels, 21, 1792–1815.

Garcia-Perez M., Chaala A., Pakdel H., Kretschmer D., Roy C, 2007. Characterisation of bio-oils in chemical families. Biomass Bioenergy. 31, 222-242.

Garcia-Perez M., Shen J., Wang X. S., Li C-Z, 2010. Production and fuel properties of fast pyrolysis oil/ bio- diesel blends. Fuel Process. Technol. 91, 296-305.

Idris S.-S., Rahman N.-A., Ismail K., Alias A.B., Abd Rashid Z., Aris M.J., 2010. Investigation on thermochemical behaviour of low rank Malaysian coal, oil palm biomass and their blends during pyrolysis via thermogravimetric analysis (TGA). Bioresour. Technol. 101, 4584-4592

Lea-Langton, A., Md Zin, R., Dupont, V., Twigg, M. V., 2011. In press. Int. J. Hydrogen Energy. doi:10.1016/j.ijhydene.2011.05.083

Lin, Y-C., and Huber, G. W., 2009. The critical role of heterogeneous catalysis in lignocellulosic biomass conversion. Energy Environ. Sci., 2, 68-80.

Luangkiattikhun P., Tangsathitkulchai C., Tangsathitkulchai M., 2008. Non-isothermal thermogravimetric analysis of oil-palm solid wastes, Bioresour. Technol. 99, 986-997

Marquevich M., Farriol X., Medina F., Montane D., 2001. Hydrogen production by steam reforming of vegetable oils using nickel based catalysts. Ind. Eng. Chem. Res. 40, 4757- 4766

Nikitas, C., Boulos, S., Shokar, P., Leach, B., 2005. Review of wood waste arisings and management in the UK, Summary Report., The Waste and Resources Action Programme (WRAP). ISBN: 1-84405-201-X

Parfitt, J., 2002. Analysis of household waste composition, The Waste and Resources Action Programme (WRAP).

Pimenidou P., Rickett G.L., Dupont V., Twigg M.V., 2010a. Chemical looping reforming of waste cooking oil in a packed bed reactor. Bioresour. Technol. 101, 6389- 6397.

Pimenidou P, Rickett G.L., Dupont V. and M.V.Twigg, 2010b. High purity H_2 by sorption-enhanced chemical looping reforming of waste cooking oil in a packed bed reactor. Bioresour. Technol.. 101, 9279- 9286

Qi Z., Jie C., Tiejun W., Ying X., 2007. Review of biomass pyrolysis oil properties and upgrading research. Energy Convers. Manage. 48, 87- 92.

Qiang L., Wen-Zhi L. ,Xi- Feng Z., 2010. Overview of fuel properties of biomass fast pyrolysis oil. Energy Convers. Manage. 50, 1376- 1383.

Reina J., Velo E., Puigjaner L., 1998. Thermogravimetric study of the pyrolysis of waste wood Thermochim. Acta. 320, 161-167

Saddawi, A., Le Coeur, C., Jones, J. M. , Williams, A., 2011. Commodity fuels from biomass through pre-treatment and torrefaction – effects of mineral content on torrefied fuel characteristics and quality. International Conference on Carbon Reduction Technologies, Polish Jurassic Highland (Jura Region), Poland, 19-22 September 2011.

Sadeghbeigi, R., 2000. Fluid catalytic cracking handbook. Design, Operation and Troubleshooting of FCC facilities. Chapter 2 FCC Feed Characterization, p. 52. 2nd Edition, Butterworth-Heinemann.

Sims R.E.H., Mabee W., Saddler J.N., Taylor M., 2010. An overview of second generation biofuels technologies. Bioresour. Technol. 101, 1570-1580.

Sukiran, M. A., Chin, C. M., Abu Bakar, N. K., 2009. Bio-oils from Pyrolysis of Oil Palm Empty Fruit Bunches. Am. J. Appl. Sci. 6 (5): 869-875.

Tanaka R. and Yamamoto, K., 2002. Accumulation and availability of oil palm biomass in Malaysia. In 'Tanaka, R., and Cheng, L. H. (ed) Proc. 3rd USM-JIRCAS Joint international symposium (9-11 March 2004), Penang, Malaysia, JIRCAS working report No. 39, 20-34.

Urbanovici, E., Popescu, C., Segal E., 1999. Improved iterative version of the Coats- Redfern method to evaluate non- isothermal kinetic parameters. J. Therm. Anal. Calorim. 58, 683-700

Wan Y., Chen P., Zhang B., Yang C., Liu Y., Lin X., Ruan R., 2009. Microwave- assisted pyrolysis of biomass: Catalysts to improve products selectivity. J. Anal. Appl. Pyrolysis.86, 161-167.

Wang D., Czernik S., Montane D., Mann M., Chornet E., 1997. Biomass to hydrogen via fast pyrolysis and catalytic steam reforming of the pyrolysis oil and its fraction. Ind. Chem. Eng. Res. 36, 1507- 1518.

Wang Z. X., Dong T., Yuan L.X., Kan T., Zu X.F., Torimoto Y., Sadakata M., Li Q.X., 2007. Characteristics of bio-oil syngas and its utilization in Fischer-Tropsch synthesis. Energy Fuels. 21, 2421-2432.

Williams P.T., Horne P.A., 1995. The influence of catalyst type on the composition of upgraded biomass pyrolysis oils. J. Anal. Appl. Pyrol. 31, 39- 61.

Zhang, H., Cheng, Y-T., Vispute, T.P., Xiao R., and Huber, G.W., 2011. Catalytic conversion of biomass-derived feedstocks into olefins and aromatics with ZSM-5: the hydrogen to carbon effective ratio. Energy Environ. Sci. 4, 2297-2307.

Zhang Q., Chang J., Wang T., Xu Y., 2007. Review of biomass pyrolysis oils properties and upgrading research. Energy Convers. Manage. 48, 87-92.

Zhao C., Khou Y., Lemonidou A.A., Li X., Lercher J.A., 2009. Highly selective catalyst conversion of phenolic bio-oil to alkanes. Angew. Chem.. Ind. Ed. 48, 3987-3990.

Zhu X., Venderbosch R., 2005. A correlation between stoichiometrical ratio of fuel and its higher heating value. Fuel. 84, 1007- 1010.

Table 1 Characteristics of the bio-oils and numerical indicators for their utilisation or upgrading.

Analysis oil	'wet' pine	'wet' PEFB	mf pine	mf PEFB
Ultimate				
C (wt%-mol fr)	40.75-0.257	45.23-0.284	52.76-0.359	59.98-0.409
H (wt%-mol-fr)	6.59-0.494	6.53-0.488	5.29-0.427	5.08-0.412
N (wt%)	1.4×10^{-3}-	8.5×10^{-3}-	1.8×10^{-3}-	11.3×10^{-3}-
(mol fr)	7.6×10^{-4}	4.6×10^{-3}	1.1×10^{-3}	6.6×10^{-3}
S (wt%)	0.0436-	0.0611-	0.0564-	0.0810-
(mol fr)	1.03×10^{-4}	1.44×10^{-4}	1.44×10^{-4}	2.07×10^{-4}
K (wt%)	0.00575-	0.14176-	0.00744-	0.18801-
(mol fr)	1.1×10^{-5}	2.74×10^{-4}	1.53×10^{-5}	3.94×10^{-4}
Na (wt%)	0.00793-	0.00745-	0.01027-	0.00988-
(mol fr)	2.61×10^{-5}	2.45×10^{-5}	3.64×10^{-5}	3.52×10^{-5}
Ca (wt%)	0.04-	0.05-	0.0518-	0.0663-
(mol fr)	7.6×10^{-5}	9.4×10^{-5}	1.06×10^{-4}	1.34×10^{-4}
Si (wt%)	0.0564-	0.0523-	0.0730-	0.0694-
(mol fr)	1.52×10^{-4}	1.41×10^{-4}	2.12×10^{-4}	2.03×10^{-4}
O (wt%-mol-fr)	52.27-0.247	47.03-0.222	41.72-0.213	33.72-0.173
Proximate				
Water (wt%)	22.55	24.30	0	0
Volatiles (wt%)	86.6-88.2	84.3-88.7	65.6-66.1	41.3-60.0
Carbon rsd(wt%)	11.8-13.4	11.3-15.7	33.9-34.4	40-58.7
Ash (wt%)	3.78	2.43	4.89	3.22
HHV $_{b.c.}$ (MJ/kg)	15.6	19.8	20.14	26.18
HHV (Zhu)(MJ/kg)	14.53	16.99	23.4	27.6
HHV (Chan) (MJ/kg)	16.5	18.5	20.3	23.4
LHV $_{b.c.}$(MJ/kg)	14.2	18.4	19.0	25.1
$H_{f,25°C\ b.c.}$(MJ/kg)	-38.3	-43.9	-44.9	-53.0
Numerical Indicators				
Max H_2 yield (wt %)	13.7	15.9	17.7	21.0
$(H/C)_{eff}$	-0.01	0.11	0.0	0.11
x=Ca/Si (mol fr)	0.50	0.67	0.50	0.67
Af (mol/GJ)	-1.75	-0.64	-1.69	-0.58
S/(K+Na) (mol fr)	2.76	0.48	2.76	0.48

Table 2 Initial and final temperatures (T_i, T_f) and respective mass losses for phases 1 and 2 (PH1, PH2) during TGA of the bio-oils under heating rate β.

oil	β	Mass loss (%)		T_i (K)		T_f (K)	
	(K min^{-1})	PH1	PH2	PH1	PH2	PH1	PH2
Pine	3	44	36	279	396	396	779
Pine	6	48	35	279	411	411	719
Pine	9	42	45	281	398	398	896
EFB	3	30	60	304	368	368	629
EFB	6	29	61	299	372	372	636
EFB	9	20	70	307	377	377	667

Table 3 Best fit model, kinetic parameters (E,A,n), correlation coefficient of linearity (r) and temperature range of application of the model (Temp. Fit) for phases PH1 and PH2 of the bio-oils' thermal degradation in TGA with heating rate β.

oil	PH	β	Model	$E\pm dE$	$\ln A\pm d\ln A$			Temp.
		K min^{-1}	$g(\alpha)$	(kJ mol^{-1})	(A in s^{-1})	(n)	(r)	Fit (K)
Pine	PH1	3	Reac.ord	78.1±0.3	23.3 ± 0.1	2.9	0.995	282-362
Pine	PH1	6	Reac.ord	63.8±0.3	17.6 ± 0.1	2.3	0.993	281-386
Pine	PH1	9	Reac.ord	68.5±33.1	19.6 ± 0.1	3	0.985	283-390
Pine	PH2	3	Reac.ord	70.7±0.1	13.9±0.1	6.6	0.993	368-546
Pine	PH2	6	Reac.ord	49.4 ±0.1	7.32 ±6	4.2	0.987	378-600
Pine	PH2	9	Reac.ord	45.2 ± 0.2	6.13± 0.1	3.8	0.984	385-608
EPFB	PH1	3	Reac.ord	26.9±0.6	1.5±0.2	2.9	0.989	303-367
EPFB	PH1	6	3D diff	56.6±1.0	9.3±7.4	N/A	0.986	299-375
EPFB	PH1	9	3D diff	55.4±1.4	7.9±7.5	N/A	0.989	307-378
EPFB	PH2	3	3D diff	15.8±0.1	-4.9±5.8	N/A	0.998	367-628
EPFB	PH2	6	3D diff	15.4±0.2	-5.1±5.8	N/A	0.998	375-636
EPFB	PH2	9	3D diff	20.3±0.2	-4.1±6.1	N/A	0.996	378-667

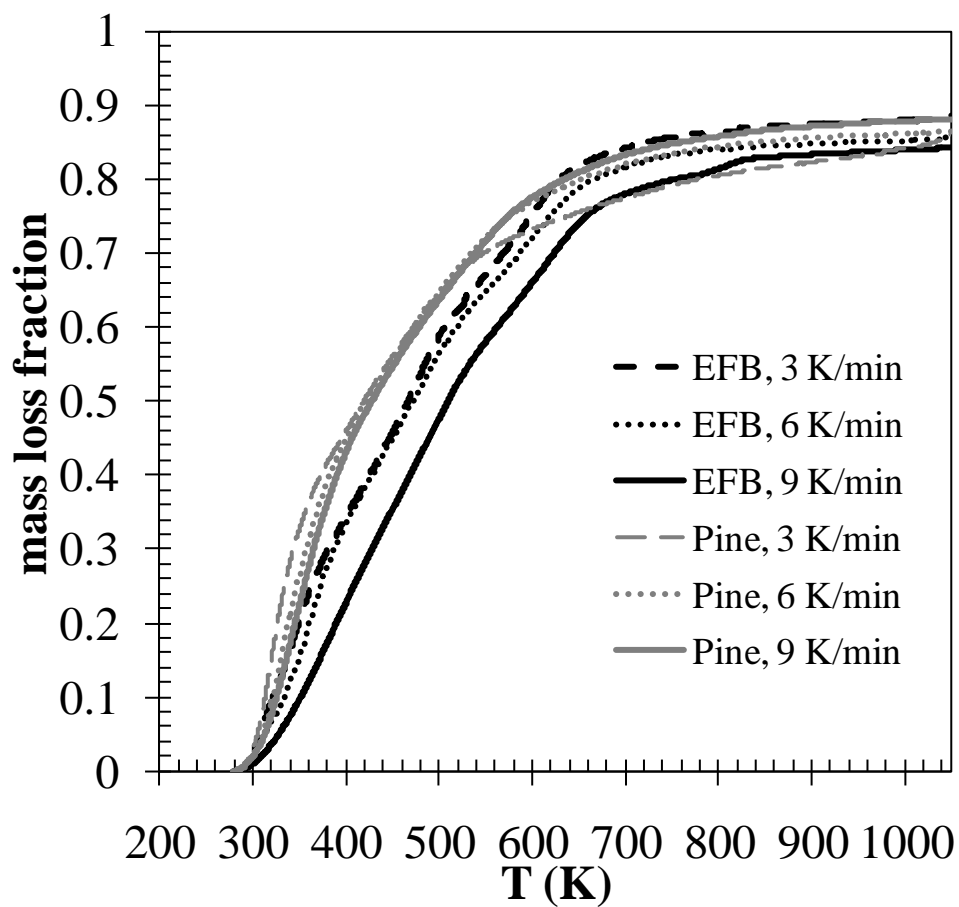**Fig. 1.** TGA mass loss fraction $\left(\dfrac{m_{t=0} - m_t}{m_{t=0}}\right)$ for as-received EPFB and pinewood oil in a flow of 50 mL min^{-1} N$_2$ at different heating rates, up to 1073 K.
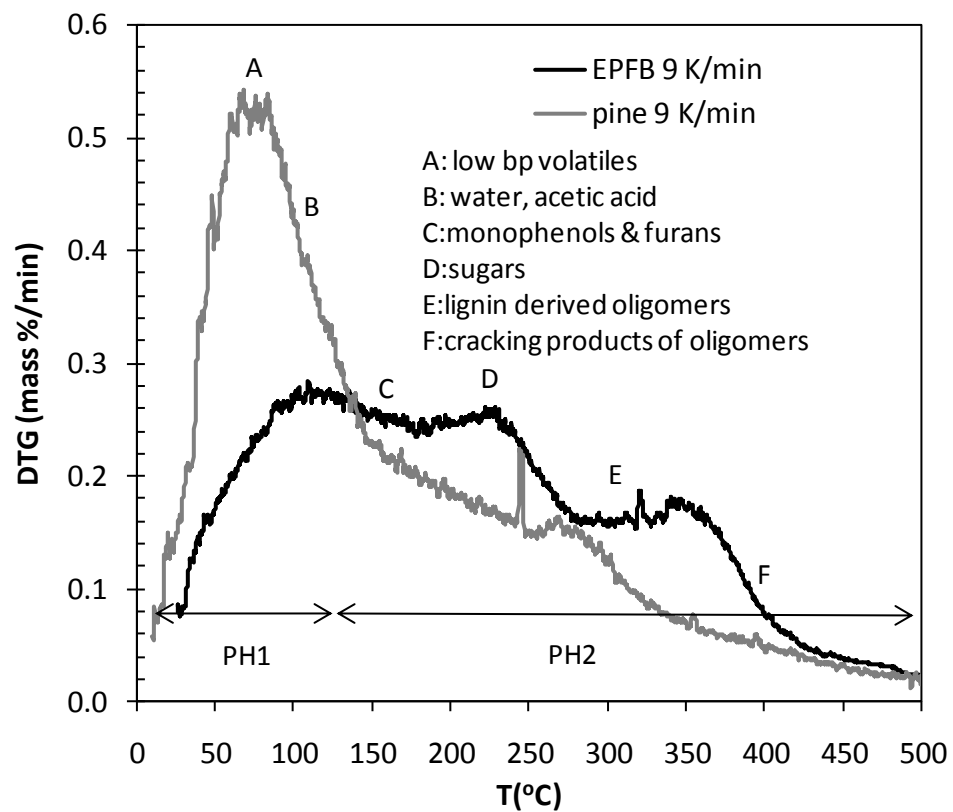
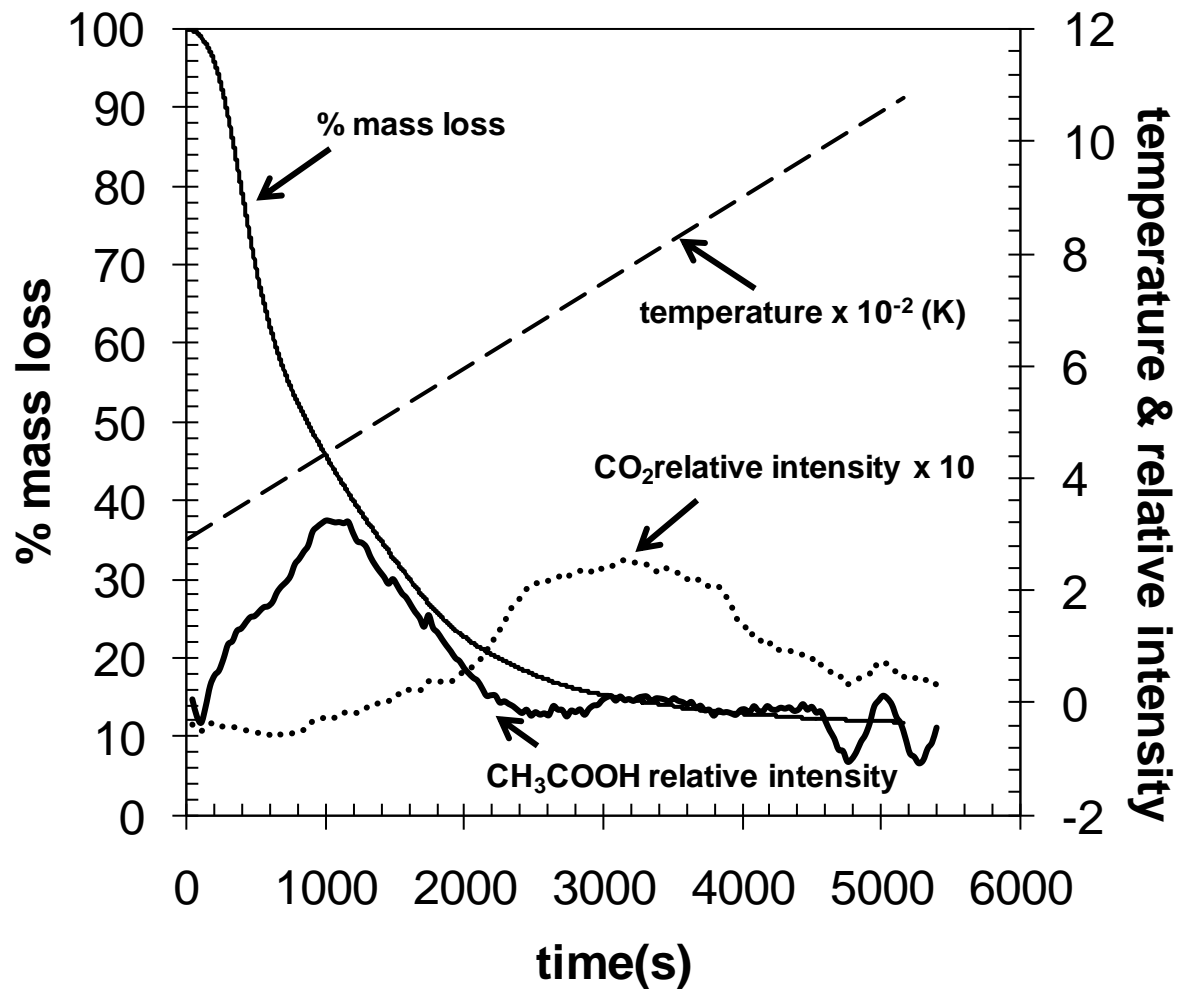Fig. 2 DTG vs. temperature curves for as-received PEFB and pine oils at 9K/min

Fig. 3. TGA curve and relative intensity of acetic acid and CO_2 from the FTIR spectra of as-received pinewood oil at 9 K min^{-1}.
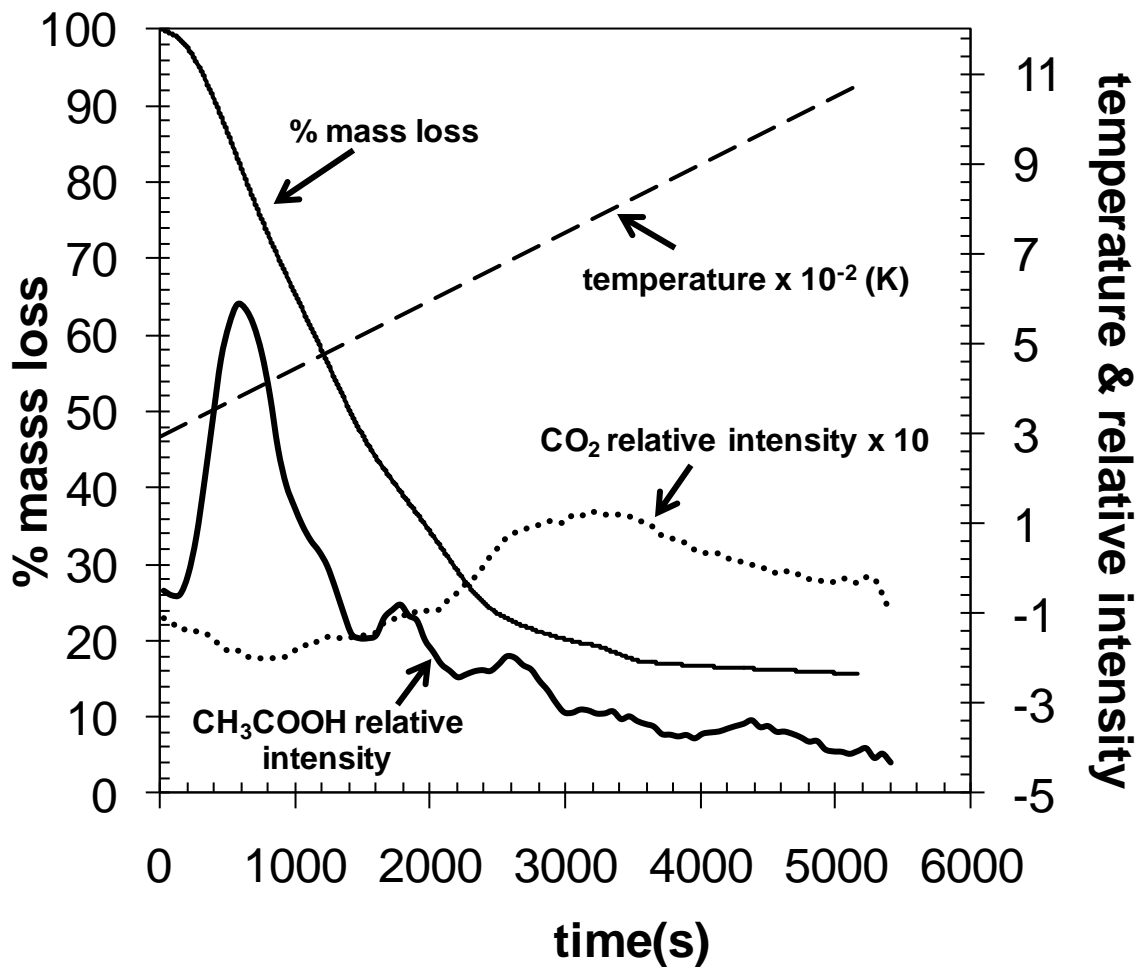
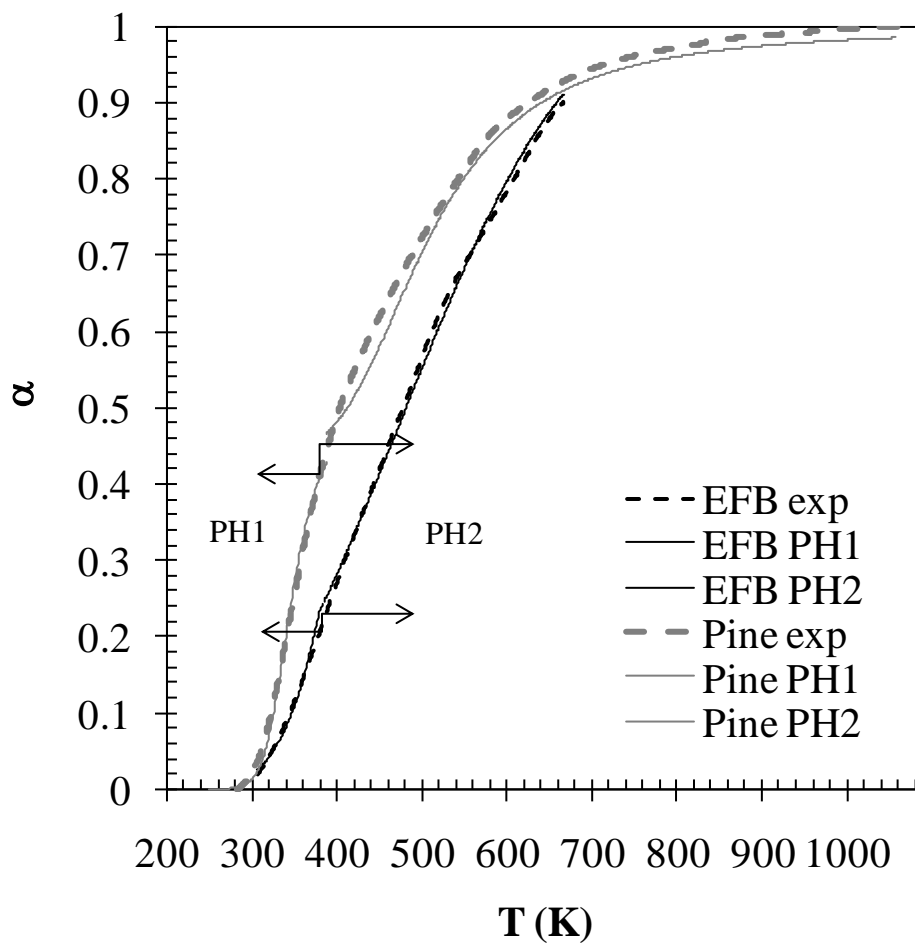**Fig. 4.** As Fig. 3 for as-received PEFB oil.

Fig. 5. TGA renormalized experimental and modelled conversion curves for PH1 and PH2 using the reaction order model for the as-received pinewood oil and the 3D 'Jander' diffusion model for the as-received PEFB oil at heating rate of 9 K min^{-1} for both oils.